Thermal rectifying effect in two-dimensional anharmonic lattices

Jinghua Lan
Department of Physics and Centre for Computational Science and Engineering, National University of Singapore, Singapore 117542

Baowen Li*
Department of Physics and Centre for Computational Science and Engineering, National University of Singapore, Singapore 117542;
Laboratory of Modern Acoustics and Institute of Acoustics, Nanjing University, 210093, People's Republic of China;
and NUS Graduate School for Integrative Sciences and Engineering, Singapore 117597, Republic of Singapore
(Received 7 July 2006; revised manuscript received 26 September 2006; published 29 December 2006)

We study thermal rectifying effect in two-dimensional systems consisting of the Frenkel Kontorva lattice and the Fermi-Pasta-Ulam lattice. It is found that the rectifying effect is related to the asymmetrical interface thermal resistance. The rectifying efficiency is typically about two orders of magnitude which is large enough to be observed in experiment. The dependence of rectifying efficiency on the temperature and temperature gradient is studied. The underlying mechanism is found to be the match and mismatch of the spectra of lattice vibration in two parts.

DOI: 10.1103/PhysRevB.74.214305 PACS number(s): 67.40.Pm, 63.20.Ry, 66.70.+f, 44.10.+i

I. INTRODUCTION

Heat conduction in low dimensional systems has attracted increasing attention[1–23] in recent years. After two decades of analytic and numerical studies in the one-dimensional (1D) model, much progress has been achieved. On the one hand, the study has enriched our understanding about the underlying physical mechanism. On the other hand, the study has made it possible to seek the practical application of heat control and management. Indeed, in 2002, Terraneo *et al.*[24] proposed a thermal device which can rectify the heat current through it when reversing the temperature gradient. The model proposed by Terraneo *et al.* is a 1D anharmonic lattice consisting of three segments with the Morse on-site potential of different parameters. As the first attempt of controlling heat current, the ratio of the thermal current changes is less than two. More recently, Li *et al.*[25] constructed a thermal diode model in which two Frenkel-Kontoroval (FK) chains with different nonlinear strengths are connected by a harmonic spring. The most successful improvement of the model by Li *et al.*[25] lies in three facts: First, the configuration is more simple, it consists of only two different segments; second, the ratio of heat current from two different directions is increased drastically about 100 times; and third, the underlying mechanism of thermal rectifying effect is explained by illustrating the phonon bands of the particles in different segments. Following Li *et al.*'s work, we further improve the rectifying efficiency from 100 to 2000 by substituting the weak FK chain with a Fermi-Pasta-Ulam (FPU) chain.[26] In addition, we find that the rectifying effect (asymmetric heat flow) is closely related to asymmetric interface thermal resistance (also called Kapitza resistance). Moreover, a specific relationship between the ratio of heat current and the overlap of the phonon spectra is demonstrated numerically. The rectifying effect can also be achieved by modulating the periodicity of the on-site potential of the FK lattice.[27]

The above works demonstrate the possibility of controlling heat current by changing structures/parameters of anharmonic lattices. These might find potential application in energy saving material. However, almost all works so far are focused on 1D systems of finite size. Obviously, much progress has been achieved, but the final purpose is to put these ideas to application. It is thus a natural step forward to seek effective thermal devices to control heat current in higher dimension. The open questions are whether the heat control mechanism in 1D is still valid for the high dimension(s) and whether the extra dimension(s) reduces the rectifying efficiency? The answer might not be trivial, as in higher dimension the lattice vibration includes not only the longitudinal one but also the transverse ones. The longitudinal modes will couple to the transverse modes,[28] which might affect the rectifying efficiency.

In this paper, we concentrate our study on a two-dimensional (2D) rectifier model. We will demonstrate with numerical evidence that a 2D rectifier can be built up and it works in a very wide temperature range. The 2D thermal rectifier shows similar behaviors with 1D thermal rectifier under similar parameters regimes.

The paper is organized as the follows. In Sec. II, we describe our model and numerical method used for the computer simulation. In Sec. III, we demonstrate and discuss the dependence of the thermal rectifying efficiency on the temperature and the temperature gradient. Section IV is devoted to the interface thermal resistance which is the key point to understand the thermal rectifying effect. In Sec. V, we give physical understanding of the rectifying effect in terms of the lattice vibration spectra (also called phonon band). We conclude the paper by conclusions and discussions in Sec. VI.

II. MODEL AND METHODOLOGY

In our previous work[26] we construct a 1D thermal diode model by connecting a FK lattice to a FPU lattice with a weak harmonic spring. We denote it as a 1D-FK-FPU model. This model displays a very good rectifying effect. In this paper, we extend the 1D-FK-FPU thermal rectifier model to a two-dimensional one. We denote it as a 2D-FK-FPU model. The configuration of the 2D-FK-FPU model is illustrated in Fig. 1. The left part is a plane of harmonic oscilla-

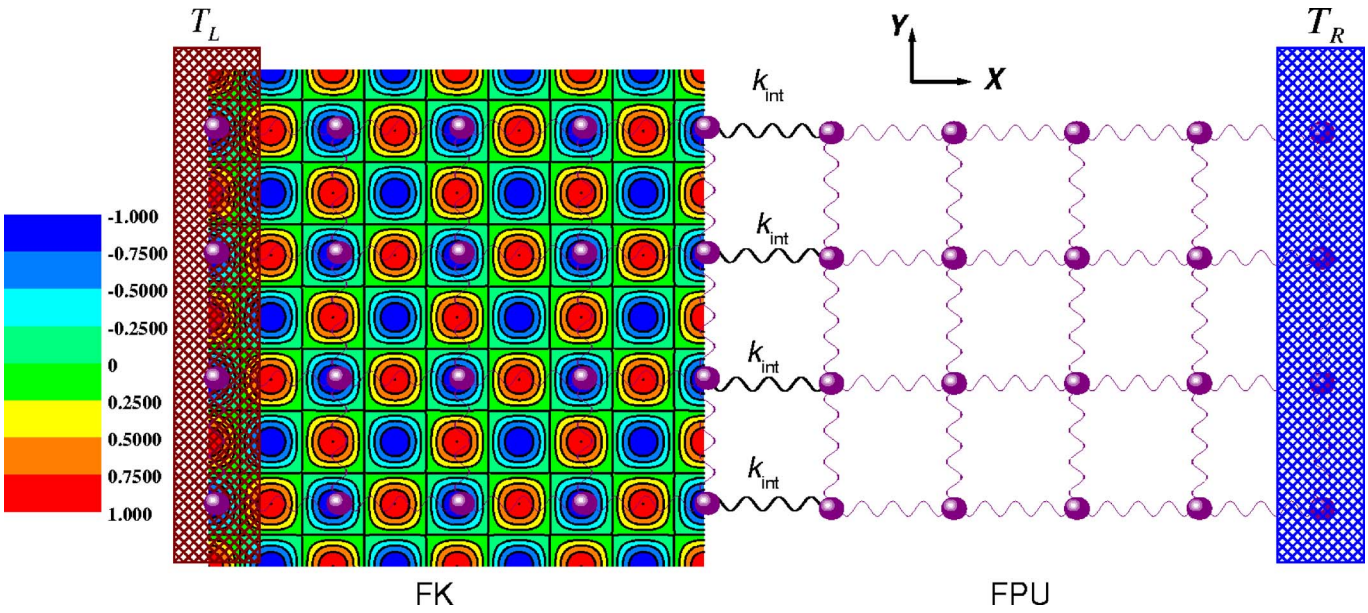

FIG. 1. (Color online) Configuration of a two-dimensional (2D) thermal rectifier from the Frenkel Kotoroval and the Fermi-Pasta-Ulam lattices. The left part is a 2D FK lattice and the right one is a 2D Fermi-Pasta-Ulam lattice. The two parts are connected by harmonic springs with constant k_{int}. The left and the right ends are put into contact with heat baths of temperature T_L and T_R, respectively.

tors on a substrate whose interaction is represented by a sinusoidal on-site potential. Here we plot the contour line of the 2D sinusoidal potential. For simplicity, we put one particle in each valley. The right part is an array of anharmonic oscillators represented by the FPU model. The two parts are connected by weak harmonic springs. The Hamiltonian of the system can be written as

$$H = H_{FK} + H_{FPU} + H_{int}, \tag{1}$$

where H_{FK}, H_{FPU}, and H_{int} are the Hamiltonian of the left part, the right part, and the interface section, respectively. They are represented in Eqs. (2)–(4), respectively.

$$H_{FK} = \sum_{i=1}^{N_{FK}} \sum_{j=1}^{N_Y} \left(\frac{\vec{p}_{i,j}^2}{2} + k_{FK} V_H(|\vec{r}_{i,j;i-1,j}| - l_0) + k_{FK} V_H(|\vec{r}_{i,j;i,j-1}| - l_0) + U_{FK}(x_{i,j}, y_{i,j}) \right), \tag{2}$$

$$H_{FPU} = \sum_{i=N_{FK}+1}^{N_X} \sum_{j=1}^{N_Y} \left(\frac{\vec{p}_{i,j}^2}{2} + k_{FPU} V_{FPU}(|\vec{r}_{i,j;i-1,j}| - l_0) + k_{FPU} V_{FPU}(|\vec{r}_{i,j;i,j-1}| - l_0) \right), \tag{3}$$

$$H_{int} = \sum_{j=1}^{N_Y} k_{int} V_H(|\vec{r}_{N_{FK},j;N_{FK}+1,j}| - l_0), \tag{4}$$

where $\vec{r}_{i,j;k,l} = \vec{q}_{i,j} - \vec{q}_{k,l}$ is the relative displacement between particles, labeled as (i,j) and (k,l). $V_H(x) = \frac{1}{2}x^2$, $V_{FPU}(x) = \frac{1}{2}x^2 + \frac{1}{4}x^4$, and $U_{FK}(x,y) = -\frac{A}{(2\pi)^2}\cos\left(\frac{2\pi}{l_0}x\right)\cos\left(\frac{2\pi}{l_0}y\right)$.

The mass of the particles is uniformly 1. l_0 is the distance between nearest neighbors in equilibrium. The particle at the ith column and the jth row is labeled as (i,j). The coordinate and momentum of this particle is $\vec{q}_{i,j} = (x_{i,j}, y_{i,j})$ and $\vec{p}_{i,j} = (p_{x_{i,j}}, p_{y_{i,j}})$. In order to establish a temperature gradient, the two ends of the planes are put into contact with two Nosé-Hoover heat baths[29] with temperature T_L and T_R for the left end and the right end, respectively. Particles for $i=1$, $j = 1,2,3,\ldots,N_Y$ are coupled with a heat bath of temperature T_L and particles for $i=N_X$, $j=1,2,3,\ldots,N_Y$ are coupled with a heat bath of temperature T_R. We checked in the 1D case that the result does not depend on the particular heat bath realization. A fixed boundary condition is used along temperature gradient direction, denoted as X direction in this paper, namely, $\vec{q}_{0,j} = (0,j)$, $\vec{q}_{N_X+1,j} = (N_X+1,j)$. A periodic boundary condition is applied in the Y direction, namely, $\vec{q}_{i,1} = \vec{q}_{i,N_Y+1}$ (see Fig. 1). Under these boundary conditions, the system can be considered as a tube. The total number of particles is $N_X \times N_Y$. All results given in this paper are obtained by averaging over $N \times 10^8 (N > 2)$ steps after a sufficient long transient time when a nonequilibrium stationary state is set up. The equations of motion of the particles are

$$\dot{\vec{q}}_{i,j} = \vec{p}_{i,j},$$

$$\dot{\vec{p}}_{i,j} = \begin{cases} -\dfrac{\partial H}{\partial \vec{q}_{i,j}} (i = 2, N_X - 1), \\ -\dfrac{\partial H}{\partial \vec{q}_{i,j}} - \xi_{i,j}\vec{p}_{i,j} (i = 1, N_X), \end{cases} \tag{5}$$

and the auxiliary variables $\xi_{i,j}$ are described by the equation

$$\dot{\xi}_{i,j} = \frac{1}{\mathcal{Q}}\left(\frac{\vec{p}_{i,j}^2}{2k_BT} - 1\right), \tag{6}$$

here, T is the temperature of the heat bath (T_L or T_R), and $\mathcal{Q}$ is the parameter of coupling between the thermal bath and the system. In this study, we set $\mathcal{Q}=1$ so that the response time of the thermostats, $\frac{1}{\sqrt{\mathcal{Q}}}$, is of the same order of the original time scale of the lattice. Our purpose is to study rectifying effect in two dimension and the dependence of the rectifying efficiency on the system temperature and the temperature gradient, so we do not attempt to search the optimum setting of parameters. We choose the system parameters the same as in the 1D-FK-FPU model which has been tested as a good one in the 1D case, that is $k_{FK}=1$, $A=5$, $l_0=1$, $k_{FPU}=0.2$, and $k_{int}=0.05$. We set

$$T_L = T_0(1+\Delta),$$

$$T_R = T_0(1-\Delta), \tag{7}$$

where $-0.8 \leqslant \Delta \leqslant 0.8$ in our simulations. So we can simply denote T_0 as the temperature added on the system and $2\Delta = (T_R - T_L)/T_0$ as the normalized temperature difference of the system.

The temperature used in our numerical simulation is dimensionless. It is connected with the true temperature T_r through the following relation:[9] $T_r = \frac{m\omega_0^2 b^2}{k_B}T$, where m is the mass of the particle and b is the period of external potential. ω_0 is the vibration frequency. k_B is the Boltzman constant. For the typical values of atoms, we have $T_r \sim (10^2 - 10^3)$,[9] which means that the room temperature corresponds to the dimensionless temperature $T \sim (0.1-1)$.

The local temperature is defined as

$$T_{i,j} = \frac{1}{2}m\langle \vec{v}_{i,j}^2 \rangle, \tag{8}$$

where $\langle \cdots \rangle$ stands for a temporal average. The local heat current $J_{i,j}$ is defined as the energy transfer per unit time from the particle labeled as (i,j) to the nearest particles along the X direction.

$$J_{i,j} = -\vec{v}_{i,j} \cdot \vec{F}_{i,j}$$
$$= -k\vec{v}_{i,j} \cdot \frac{\partial[V(|\vec{r}_{i+1,j;i,j}| - l_0) + V(|\vec{r}_{i,j;i-1,j}| - l_0)]}{\partial \vec{q}_{i,j}}, \tag{9}$$

where $k=k_{FK}$, k_{FPU}, or k_{int}, depending on the site along the X direction. For a 2D lattice, we treat only heat current flowing along the X direction. We denote the current from the particles in the ith section to the next section in the X direction simply as $J_i (J_i = \Sigma_{j=1}^{N_Y} J_{i,j})$. The total current of the system is averaged over all sections,

$$J = \frac{1}{N_X}\left\langle \sum_{i=1}^{N_X} J_i \right\rangle. \tag{10}$$

In our simulations, the fluctuations of temporal heat current through each section are all less than 5%. We use $|J_+/J_-|$ as a *rectifying efficiency* to describe quantitatively the rectifying performance of the system. J_+ is the current when Δ is positive (heat flows from the FK part to the FPU part) and J_- is the current when Δ is negative (heat flows from the FPU part to the FK part).

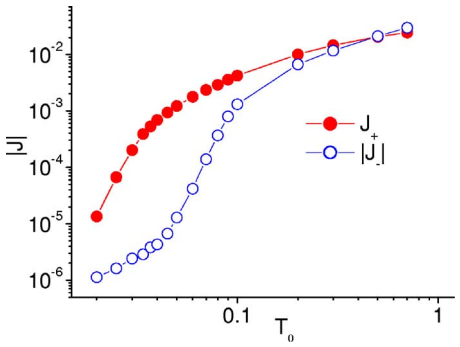

FIG. 2. (Color online) Heat current of the system with $N_Y=4$ and $N_X=10$ vs T_0. $|\Delta|=0.5$.

The model we used is a simple extension from one dimension to two dimension, however the results in Fig. 2 show that it truly demonstrates good rectifying effect on heat current. In Fig. 2, we can see the visible difference between J_+ and J_- in a very wide temperature range. The difference varies from a few times to several hundreds times.

III. DEPENDENCE OF RECTIFYING EFFECT ON TEMPERATURE AND TEMPERATURE DIFFERENCE

In this section, we study the dependence of the system performance on the temperature change. Figure 3 shows the rectifying efficiency $|J_+/J_-|$ versus T_0. In Fig. 3(a), we can see that there exists an optimum performance (OP) of the rectifying effect when changing temperature T_0. We can define the temperature for the optimum performance as T_{OP}. In Figs. 3(b)–3(d) we show the dependence of the ratio $|J_+/J_-|$ on temperature under different conditions. We found that T_{OP} depends on the system settings along the Y direction. In Fig. 3(b), the number of particles along the Y direction varies from 4 to 8 and 16 while other settings are kept unchanged. We can see clearly that T_{OP} shifts to lower temperature when increasing N_Y. The value of T_{OP} is 0.04, 0.037, and 0.0325 for $N_Y=4$, 8, and 16, respectively. T_{OP} keeps the same value when we change N_X. This is shown in Fig. 3(c). In Fig. 3(d), we change the periodic boundary condition in the Y direction to a free boundary condition. T_{OP} and the optimum performance change drastically. T_{OP} changes from 0.037 to 0.025 and the ratio increases almost 100%.

Quantity W_T in the figures is a parameter defined as the width of the effective temperature range T_e over the half value of OP, while $\vartheta = W_T/T_{OP}$ is defined as the *quality factor*. T_e, W_T, and $\vartheta = W_T/T_{OP}$ are useful parameters to estimate the temperature range in which the system has a good rectifying effect. In our investigation, T_e broadens from the center [0.03–0.46] to high temperature region or low temperature region. The typical value of W_T under different settings is around 0.018–0.023. ϑ is always larger than 0.5. The results suggest that the system is effective in a very wide temperature range.

In Fig. 4, we show the heat current versus the (normalized) temperature difference, Δ, for three different T_0. Full

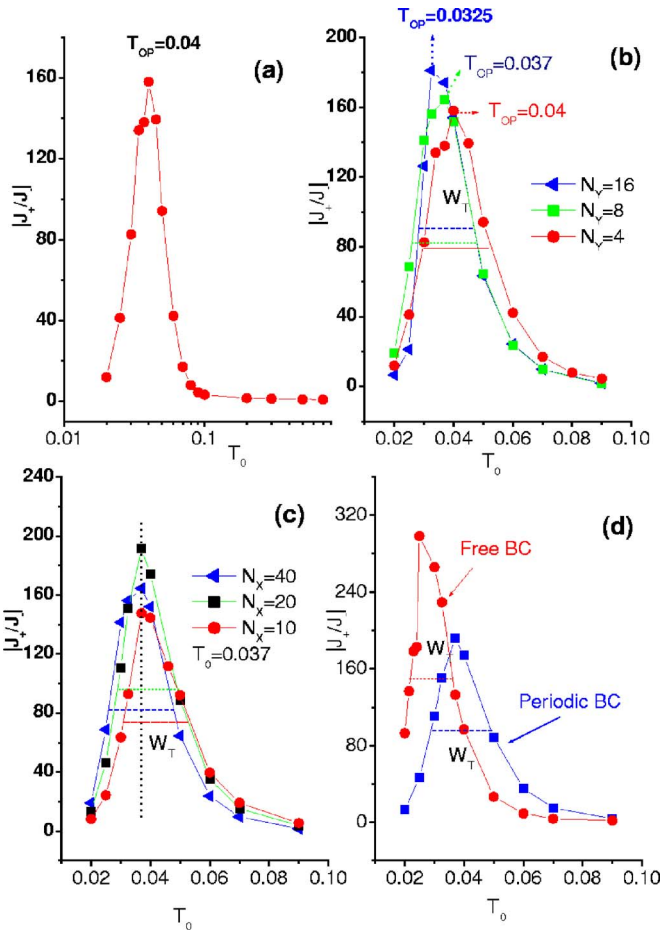

FIG. 3. (Color online) The rectifying efficiency, $|J_+/J_-|$, vs T_0 at different conditions. (a) The system with $N_Y=4$, $N_X=10$, and $|\Delta|=0.5$. $T_{OP}=0.04$. (b) Comparison for three different N_Y with $N_X=40$. $T_{OP}=0.04$, $W_T=0.022$, and $\vartheta=0.55$ for the case of $N_Y=4$. When $N_Y=8$, $T_{OP}=0.037$, $W_T=0.022$, and $\vartheta=0.59$. When $N_Y=16$, $T_{OP}=0.0325$, $W_T=0.018$, and $\vartheta=0.55$. (c) Comparison for three different N_X with $N_Y=8$. They have the same $T_{OP}=0.037$. When $N_X=10$, $W_T=0.023$, and $\vartheta=0.62$. When $N_X=20$, $W_T=0.020$, and $\vartheta=0.54$. When $N_X=40$, $W_T=0.022$, and $\vartheta=0.59$. (d) Comparison for different boundary conditions along the Y direction with $N_Y=8$, $N_X=20$. Free boundary: The optimum performance (OP) $=298.5$, $T_{OP}=0.025$, $W_T=0.014$, and $\vartheta=0.56$. Periodic boundary: $OP=191.5$, $T_{OP}=0.037$, $W_T=0.022$, and $\vartheta=0.59$.

symbols represent J_+ and empty ones $|J_-|$. We can see that J_+ increases with Δ monotonically and it is always larger than $|J_-|$, while J_- changes with Δ in different ways. One can find that there are three regions for $|J_-|$. In the first region, $|\Delta|<0.1$, the increase of Δ leads to the increase of the heat current. However, in the second region, $0.1<|\Delta|<0.6$, the increase of $|\Delta|$ does not induce the increase of $|J_-|$, instead it results in a decrease of $|J_-|$. In the third region, $\Delta>0.6$, $|J_-|$ is almost a constant independent of $|\Delta|$. In this region, the $|J_-|$ is so small that the system can be approximately considered as an insulator. The ratio $|J_+/J_-|$ becomes larger and larger when $|\Delta|$ increases. That indicates that rectifying effect increases with increasing temperature difference.

The strange behavior of $|J_-|$ observed in the second region, namely, the larger the temperature difference the smaller the heat current, is called *negative differential thermal resistance*. We will demonstrate later that this is a typical phenomenon in nonlinear lattices. It can be understood from the match and mismatch of the vibrational spectra of the interface particles.

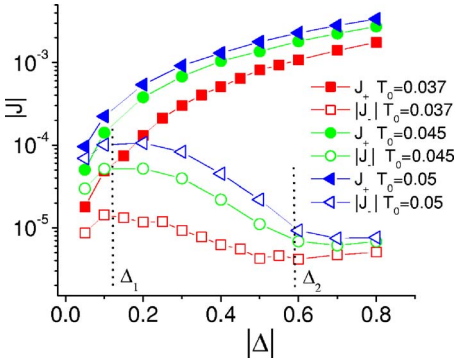

FIG. 4. (Color online) Heat current of the system with $N_Y=8$, $N_X=20$ vs temperature difference at three different T_0. Note that $|J_-|$ decreases as $|\Delta|$ increases in the interval $0.1<|\Delta|<0.6$, this is the so-called "*negative differential thermal resistance*," see text for more explanation.

Figure 5 shows $|J_+/J_-|$ versus $|\Delta|$. It is found that $|J_+/J_-|$ increases with $|\Delta|$ in an exponential way in the regime in which $|\Delta|$ is smaller than Δ_2. Approximately,

$$|J_+/J_-| \propto \exp(c * |\Delta|) + \delta, \tag{11}$$

here c is about 9.5 under the particular parameter setting $N_Y=8$ and $N_X=20$ with the periodic boundary condition along the Y direction. When we change N_Y, N_X, or the boundary condition along the Y direction, c changes slightly, but it is always around 10. The variation of $|c-10|$ is smaller than 0.5 in our investigation. δ is related with T_0 and Δ.

IV. INTERFACE THERMAL RESISTANCE (ITR)—KAPITZA RESISTANCE

Thermal resistance between two different materials or between twin or twist boundaries of the same material has been extensively studied both experimentally and theoretically.[30–33] In fact, the existence of a thermal boundary

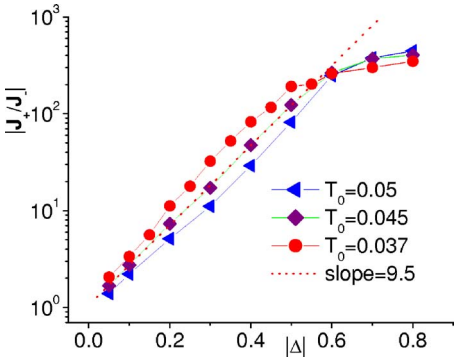

FIG. 5. (Color online) The ratio of heat current $|J_+/J_-|$ vs half normalized temperature difference $|\Delta|$ at temperature $T_0=0.037$, 0.045, and 0.05. The dotted line has a slope of 9.5.

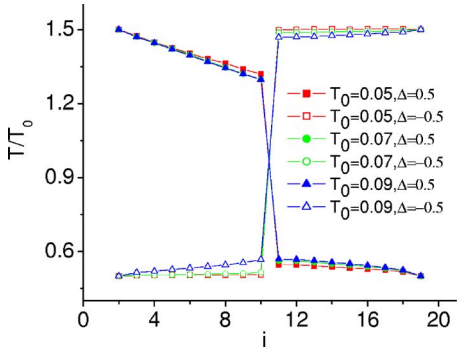

FIG. 6. (Color online) T/T_0 vs lattice site for T_0=0.05, 0.07, and 0.09. The solid symbols are for the cases of Δ=0.5 and the empty symbols are for the cases of Δ=−0.5. N_Y=8, N_X=20.

resistance between a solid and superfluid helium was first detected by Kapitza[33] as early as 1940's. This boundary resistance is named Kapitza resistance after him. Later, it is found that such a Kaptiza resistance exists at the interface between any pair of dissimilar materials. Khalatnikov[34] developed the acoustic mismatch model to explain the Kapitza resistance. Since then, continuous efforts have been devoted to this problem. More information can be found in the review by Swartz and Pohl.[35]

The Kapitza resistance is defined as

$$R = \Delta T/J, \tag{12}$$

where J is the heat current and ΔT the temperature difference between two sides of the interface.

In our system, the temperature drops are different when the temperature gradient of the system is reversed as shown in Fig. 6. Therefore we use R_+ and R_- to denote the interface resistance for the case of $\Delta > 0$ and $\Delta < 0$, respectively.

In Figs. 7 and 8, we show the dependence of IRT on temperature T_0 and the normalized temperature difference Δ. From the two figures we can see that, generally, R_- (with larger temperature drop) is about two or three orders of magnitude larger than R_+ (with smaller temperature jump). Both R_+ and R_- decrease with T_0 until $T_0 \approx 0.2$, then both become approximately constants. In Fig. 7(b), we show the ratio R_-/R_+ versus temperature T_0. It is clearly seen that there exists an optimal temperature value for the ratio R_-/R_+. In Fig. 8, we show the resistance versus temperature difference. We can see that R_- monotonically increases with temperature difference until it reaches a maximum value, while R_+ monotonically decreases with increasing Δ. If we plot the ratio of R_- over R_+ versus temperature difference, we find that the relationship between them also obeys the exponential law like the ratio of heat current.

Comparing Figs. 7 and 8 with Figs. 3 and 5, we can find that the behaviors of the IRT and heat current through the system are very similar, both are asymmetric and both the ratio R_-/R_+ and J_+/J_- have an optimum value under different temperature and obey exponential law when changing temperature difference. The asymmetry of thermal resistance when reversing temperature gradient is the determinant factor for the rectifying effect on heat current of the system from the formula (12).

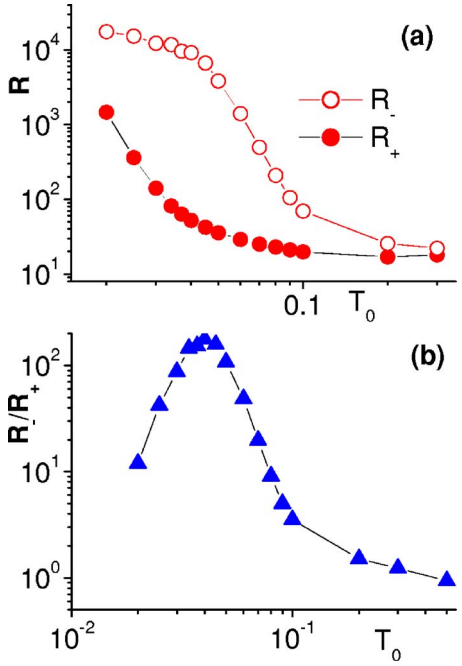

FIG. 7. (Color online) (a) Interface thermal resistance $R_\pm$ vs T_0. $|\Delta|$=0.5. (b) The ratio R_-/R_+ vs T_0. N_Y=4, N_X=10.

V. PHYSICAL MECHANISM OF RECTIFYING EFFECT: AN ANALYSIS OF LATTICE VIBRATION SPECTRUM

From the above investigation, we know that the asymmetric interface thermal resistance determines the asymmetry of heat current when reversing temperature gradient on the sys-

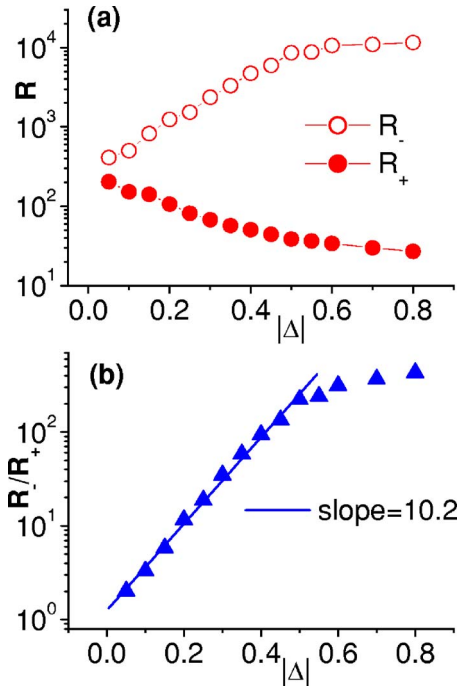

FIG. 8. (Color online) (a) $R_\pm$ vs the normalized temperature difference $|\Delta|$. T_0=0.037. (b) The ratio R_-/R_+ vs $|\Delta|$. N_Y=8, N_X=20.

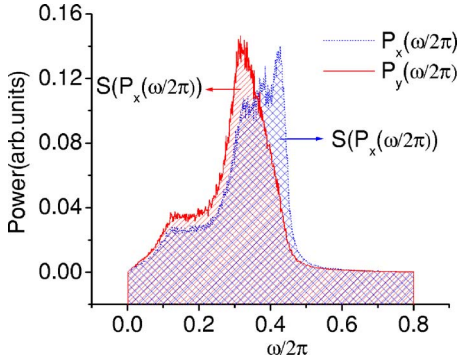

FIG. 9. (Color online) DFFT of v_x, v_y. The shadowed regions represent the integral of the power spectra. $2S[P_x(\omega/2\pi)/L] = 0.05 = \langle v_x^2 \rangle \approx T$, $2S[P_y(\omega/2\pi)/L] = 0.05 = \langle v_y^2 \rangle \approx T$.

tem, but what causes the asymmetrical behavior of the ITR? In this section, we will answer this question from a fundamental point of view: lattice vibration spectrum. Lattice vibration is responsible to heat transport in our model. An effective way to get the spectrum of lattice thermal vibration is the discrete faster Fourier transform (DFFT) for the lattice velocity.[36]

In our model, the vibration has two components, v_x and v_y. We can use the theorem of equipartition of energy to simplify the numerical calculation. According to the equipartition theorem, the molecules in thermal equilibrium (here we have local thermal equilibrium) have the same average energy associated with each independent degree of freedom of their motion and that energy is $k_B T/2$. For our system, we have $m\langle \mathbf{v}^2 \rangle/2 = k_B T$, $m\langle v_x^2 \rangle/2 = m\langle v_y^2 \rangle/2 = k_B T/2$.

In our calculation, $m=1$, $k_B=1$. So we have $\langle v_x^2 \rangle = \langle v_y^2 \rangle = T$. If we do the DFFT of v_x and v_y separately, we should have $\Sigma_{i=0}^{L-1} |v_x(t)|^2 = \Delta f \Sigma_{j=0}^{L/2-1} 2|P_x(j)|^2$ and $\Sigma_{i=0}^{L-1} |v_y(t)|^2 = \Delta f \Sigma_{j=0}^{L/2-1} 2|P_y(j)|^2$. Here $P(f)$ is the Fourier transform of velocity $v(t)$. From the equipartition theorem, one has $\Sigma_{i=0}^{L-1} |v_x(t)|^2/L = \langle v_x^2 \rangle$ and $\Sigma_{i=0}^{L-1} |v_y(t)|^2/L = \langle v_y^2 \rangle$. From the above analysis, we have $\Delta f \Sigma_{j=0}^{L/2-1} 2|P_x(j)|^2/L = T$, $\Delta f \Sigma_{j=0}^{L/2-1} 2|P_y(j)|^2/L = T$. The power spectra of vibration obtained from DFFT of v_x and v_y agree with the above formula very well (see Fig. 9). The integral of power spectra is exactly equal to the temporal average of v_x^2 and v_y^2 individually. There is a slight difference between $\langle v_x^2 \rangle$ and $\langle v_y^2 \rangle$. The difference might be caused by the number of sampled data or the different boundary conditions in the X, Y direction. In the formula, L should be infinite.

In our system, we find that the asymmetrical ITR and heat current are strongly related with the overlap of vibration spectra of the particles at the two sides of the interface. When the vibration spectra overlap with each other, the system behaves like a thermal conductor, while the system behaves like a thermal insulator when the vibration spectra are separated.

Physically, whether an excitation of a given frequency can be transported through a mechanical system depends on whether the system has a corresponding eigenfrequency. If the frequency matches, the energy can easily go through the system, otherwise, the excitation will be reflected. In our system, the overlap of the two spectra means that there exists common vibrational frequency in two parts of the system. The excitation (here as phonon) of such common frequency can be transported from one part to another. However, if the vibrational spectra of two parts are separated, then the excitation at any part cannot be transported to another part, because there exists no such corresponding frequency in another part. The change from overlap to separation is induced by the different temperature dependence of the vibration spectra of the two segments, which is a general feature of any anharmonic lattice.

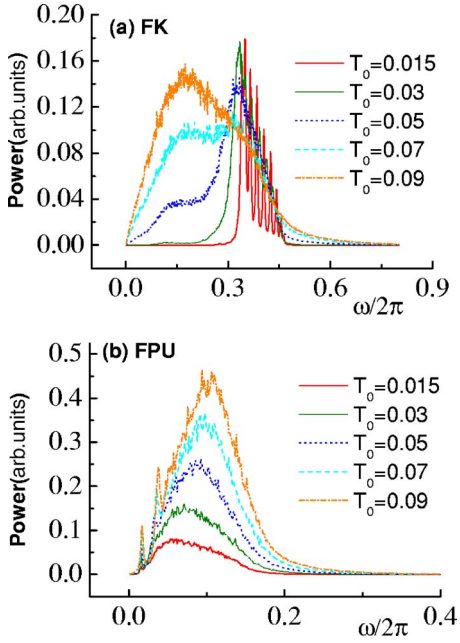

FIG. 10. (Color online) Vibration spectra of the interface particles at different temperature. (a) The vibration spectra of the particles in the FK segment. (b) The vibration spectra of the particles in the FPU segment.

In Fig. 10, we show the vibration spectra of the FK part and the FPU part under different temperatures. We can see that the vibration spectra of the FK part broaden from high frequency to low frequency when increasing the system temperature. This is because at low temperature, the atoms of the FK model are confined at the valley of the on-site potential, thus the atoms oscillate in very high frequency, however, when the temperature is increased, more and more low frequency modes can be excited. In the limiting case, when the temperature is large enough that the kinetic energy of the atom is much larger than the on-site potential, then the FK model becomes a chain of harmonic oscillators which has frequency $\omega \in [0, 2\sqrt{k_{FK}}]$.

On the contrary, the vibration spectra of the FPU part broaden from low frequency to high frequency. In fact, we have shown[26] that the highest oscillation frequency of the FPU model depends on temperature, $\omega_{FPU} \sim T^{1/4}$. Therefore, in some settings, the vibration spectra of the FK part and the FPU part will overlap with each other, while in other temperature settings, they will separate with each other. These are shown in Fig. 11. The comparison of vibration spectra of the FK part at two different temperature ranges and the FPU

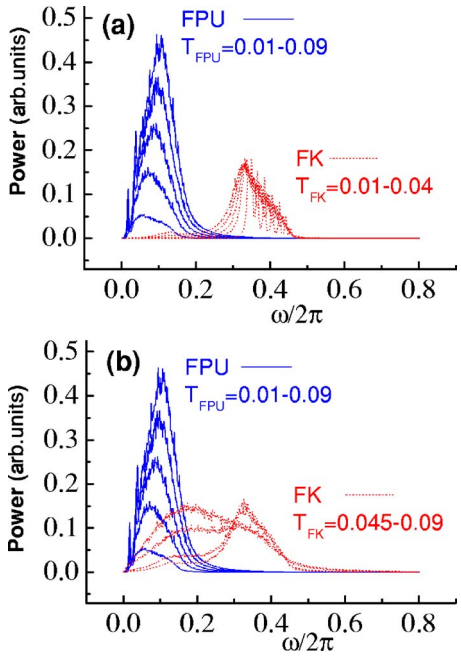

FIG. 11. (Color online) Comparison of the spectra of the FK part and the FPU part at different temperature region. (a) The spectra of the FPU part at $T_{FPU}=0.01-0.09$ (from bottom to top) and the FK part at $T_{FK}=0.01-0.04$. (b) The spectra of the FPU part at $T_{FPU}=0.01-0.09$ and the FK part at $T_{FK}=0.045-0.09$.

part at the full temperature range from 0.01 to 0.12 are shown in Figs. 11(a) and 11(b) separately. We can see that the vibration spectra of the FK part and the FPU part are matched with each other when the temperature of the FK part is from 0.05 to 0.12 [see Fig. 11(a)]. The vibration spectra of the two parts are separated from each other when the temperature of the FK part is from 0.01 to 0.03 [see Fig. 11(b)]. This indicates that when the temperature of the FK part is below a certain value, which we call T_c (0.04–0.045), the system will behave like a thermal insulator since the separated vibration spectra of the interface particles make the heat conduction almost impossible. When the temperature of the FK part is above the critical point T_c, the system will be a good thermal conductor since the matched vibration spectra allow the heat flow. Thus if we adjust T_0 and Δ appropriately to make $T_{high} \geqslant T_c$ and $T_{low} \leqslant T_c$, the system will have a good rectifying effect. If $T_{high}, T_{low} > T_c$ or $T_{high}, T_{low} < T_c$, the rectifying effect is very poor. The above analysis is based on the vibration spectra of the system with $N_Y=8$, $N_X=20$. It is consistent with the result obtained in Sec. III.

Now we look back at Fig. 3. The optimum point is at $T_0=0.037$ for $N_Y=8$, $N_X=20$, corresponding to $T_{high}=0.0505>T_c$ and $T_{low}=0.0235<T_c$. The effective temperature range T_e with $|\Delta|=0.5$ is from 0.0261 to 0.0481. The low temperatures are all smaller than T_c and all high temperatures are larger than T_c. Both decreasing T_0 and increasing T_0 in the outside region of T_e lead the system to the two extreme cases $T_{high}, T_{low} \geqslant T_c$ or $T_{high}, T_{low} \leqslant T_c$ with poor performance. From the above analysis, we can say that the different properties of heat current under different temperature and temperature difference are determined by the temperature dependence of the vibration spectra of the two segments.

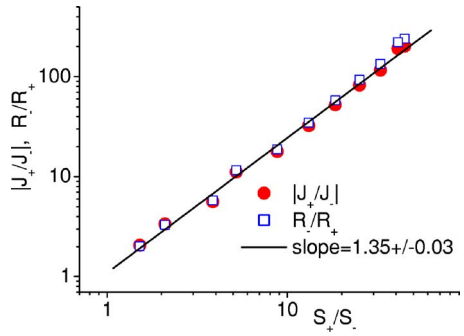

FIG. 12. (Color online) The bullets are the ratios of heat current $|J_+/J_-|$ vs S_+/S_-. Squares are the ratios of the ITR R_-/R_+ vs S_+/S_-. The dotted line has a slope 1.35 ± 0.03.

In terms of the vibration spectra of the particles in the interface, the complex behavior of $|J_-|$ in Fig. 4 can be explained from the vibration spectrum. In particular, in the range from Δ_1 to Δ_2, a novel phenomenon—called the *negative differential thermal resistance* phenomenon—is observed in Ref. 25 and fully discussed in Ref. 37. In this particular temperature interval, a larger temperature difference can induce a smaller heat current. The *negative differential thermal resistance* can be understood from the overlap and separation of the vibration spectra of the interface particles. This phenomenon is valid for a wide range of the parameters. Moreover, in Ref. 37, Li *et al.* show that it is this negative differential thermal resistance property that makes the thermal transistor possible.

More importantly, we find a specific relationship between the overlap of the vibration spectra of the two segments and the ratio R_-/R_+ in the interface or the ratio $|J_+/J_-|$ from two directions. We introduce the following quantity to describe overlap of the vibration spectra:

$$S_{\pm} = \frac{\int P_l^x(f) P_r^x(f) df}{\int P_l^x(f) df \int P_r^x(f) df} = \frac{\int P_l^x(f) P_r^x(f) df}{T_{int}^L T_{int}^R}, \qquad (13)$$

$S_{\pm}$ corresponds to the case of $\Delta>0$ and $\Delta<0$, respectively. In Fig. 12, we plot S_+/S_- versus R_-/R_+ and $|J_+/J_-|$. A very good power law was found between the ratio of resistances or heat currents and the overlap of the vibration spectra: $|J_+/J_-| \sim R_-/R_+ \propto (S_+/S_-)^{\gamma}$. The best fit for the ratio of current suggests the power law constant $\gamma=1.35\pm0.03$. Figures 11 and 12 give us a very clear and quantitative picture about the dependence of the rectifying effect of the system on the vibration spectra.

Since the rectifying effect sensitively depends on the overlap of the vibration spectra, we may find answers in Fig. 13 for the behavior of the 2D system responding to the temperature changes at different conditions. We can see clearly that when we change the number of particles in the Y direction, the temperature for the optimum performance will change, whereas when we change the number of particles in the X direction, the temperature for OP are kept at the same value; and the value of the temperature for the OP at differ-

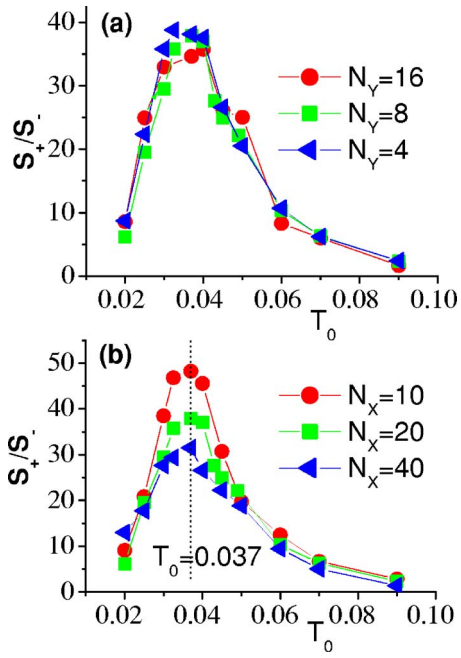

FIG. 13. (Color online) The ratio of the overlap of vibration spectra S_+/S_- vs T_0 at different conditions. (a) Comparison at three different N_Y with N_X=20. (b) Comparison at three different N_X with N_Y=8.

ent conditions found by the overlap are consistent with the value in Fig. 3. These results suggest that the different vibration spectra of the two segments and the overlap between them are the determinant factors of the system complex behaviors.

VI. DISCUSSION AND CONCLUSIONS

In this paper, we have studied the thermal rectifying effect in a 2D anharmonic lattice. The performance of the 2D thermal rectifier under different environmental changes, such as system temperature and the temperature difference on the two sides of the system, have been investigated systematically. We find that there exits an optimum performance (OP) for a specific thermal rectifier at certain temperature range. The OP is affected by the boundary condition and the number of particles, N_Y, along the Y direction. The OP shifts to lower temperature when increasing N_Y or changing the periodic boundary condition to the free boundary condition along Y direction. The 2D thermal rectifier has a good rectifying efficiency in a very wide temperature range. Another important factor that affects the performance of the thermal rectifier is the temperature difference between the two ends. We find the rectifying efficiency increases approximately as an exponential law in a certain temperature range with the temperature difference. The rectifying efficiency is mainly determined by the asymmetrical ITR. The study on the ITR shows the similar behavior with heat current.

The behaviors of the ITR and heat current of the system are strongly correlated with vibration spectra of the particles beside the interface. The asymmetry behavior of ITR and heat current is induced by the different temperature dependence of the vibration spectra of the two parts beside the interface. We find that the vibration spectra of the FK part broaden from high frequency to low frequency, conversely, the vibration spectra of the FPU part broaden from low frequency to high frequency as the temperature increases. The different temperature dependence of vibration spectra makes the system transition from a thermal conductor to an insulator possible by setting the system temperature and temperature difference properly. Moreover, a specific relationship between the performance of the system and the convolution of the vibration spectra of the two parts is found numerically as power law.

Our study on a 2D thermal rectifier gives a very clear picture about how the system responds to the environmental changes. The results should be useful for further experimental investigation. The thermal diode constructed by a monolayer thin film or a tubelike structure might have many practical applications.

ACKNOWLEDGMENTS

We would like to thank Wang Lei for helpful discussions. This work was supported in part by a FRG of NUS and the DSTA under Project Agreement No. POD0410553.

*Electronic address: phylibw@nus.edu.sg

[1] R. E. Peierls, *Quantum Theory of Solid* (Oxford University Press, London, 1955).
[2] G. Casati, J. Ford, F. Vivaldi, and W. M. Visscher, Phys. Rev. Lett. **52**, 1861 (1984).
[3] T. Prosen and M. Robnik, J. Phys. A **25**, 3449 (1992).
[4] H. Kaburaki and M. Machida, Phys. Lett. A **181**, 85 (1993).
[5] S. Lepri, R. Livi, and A. Politi, Phys. Rev. Lett. **78**, 1896 (1997).
[6] S. Lepri, R. Livi, and A. Politi, Europhys. Lett. **43**, 271 (1998).
[7] S. Lepri, Phys. Rev. E **58**, 7165 (1998).
[8] S. Lepri, R. Livi, and A. Politi, Phys. Rep. **377**, 1 (2003).
[9] B. Hu, B. Li, and H. Zhao, Phys. Rev. E **57**, 2992 (1998).
[10] A. Fillipov, B. Hu, B. Li, and A. Zeltser, J. Phys. A **31**, 7719 (1998).
[11] B. Hu, B. Li, and H. Zhao, Phys. Rev. E **61**, 3828 (2000).
[12] F. Bonetto, J. L. Lebowitz, L. Ray Bellet *et al.*, in *Mathematical Physics 2000*, edited by A. Fokas *et al.* (Imperial College Press, London, 2000), p. 128.
[13] C. Giardiná, R. Livi, A. Politi, and M. Vassalli, Phys. Rev. Lett. **84**, 2144 (2000).
[14] O. V. Gendelman and A. V. Savin, Phys. Rev. Lett. **84**, 2381 (2000).
[15] T. Prosen and D. K. Campbell, Phys. Rev. Lett. **84**, 2857 (2000).
[16] K. Aoki and D. Kusnezov, Phys. Rev. Lett. **86**, 4029 (2001).
[17] B. Li, L. Wang, and B. Hu, Phys. Rev. Lett. **88**, 223901 (2002).
[18] D. Alonso, A. Ruiz, and I. de Vega, Phys. Rev. E **66**, 066131

(2002).
[19] B. Li, G. Casati, and J. Wang, Phys. Rev. E **67**, 021204 (2003).
[20] A. Pereverzev, Phys. Rev. E **68**, 056124 (2003).
[21] B. Li and J. Wang, Phys. Rev. Lett. **91**, 044301 (2003).
[22] B. Li, G. Casati, J. Wang, and T. Prosen, Phys. Rev. Lett. **92**, 254301 (2004).
[23] N.-B. Li, P.-Q. Tong, and B. Li, Europhys. Lett. **75**, 49 (2006).
[24] M. Terraneo, M. Peyrard, and G. Casati, Phys. Rev. Lett. **88**, 094302 (2002).
[25] B. Li, L. Wang, and G. Casati, Phys. Rev. Lett. **93**, 184301 (2004).
[26] B. Li, J. Lan, and L. Wang, Phys. Rev. Lett. **95**, 104302 (2005).
[27] B. Hu and L. Yang, Chaos **15**, 015119 (2005).
[28] J.-S. Wang and B. Li, Phys. Rev. Lett. **92**, 074302 (2004); Phys. Rev. E **70**, 021204 (2005).
[29] S. Nośe, J. Chem. Phys. **81**, 511 (1984); W. G. Hoover, Phys. Rev. A **31**, 1695 (1985).
[30] H. Kinder and K. Weiss, J. Phys.: Condens. Matter **5**, 2063 (1993).
[31] T. Nakayama, in *Progress in Low Temperature Physics*, edited by D. F. Brewer (North-Holland, Amsterdam, 1989), p. 115.
[32] D. G. Cahill *et al.*, J. Appl. Phys. **93**, 793 (2003).
[33] P. L. Kapitza, J. Phys. (Moscow) **4**, 181 (1941).
[34] I. M. Khalatnikov, Sov. Phys. JETP **22**, 687 (1952).
[35] E. T. Swartz and R. O. Pohl, Rev. Mod. Phys. **61**, 605 (1989).
[36] H. P. William *et al.*, *Numerical Recipes* (Cambridge University Press, Cambridge, England, 1992).
[37] B. Li, L. Wang, and G. Casati, Appl. Phys. Lett. **88**, 143501 (2006).